

A T-type LLC Resonant DC-DC-AC Three Port Converter

Muhammad Ammar^{*1}, Muhammad Ahmed Khurshid², Prof. Dr. Tahir Mehmood³

¹Electrical Engineering Department, U.E.T Taxila, Taxila, Pakistan-muhammad.ammar3@students.uettaxila.edu.pk

²Electrical Engineering Department, U.E.T Taxila, Taxila, Pakistan.

³Electrical Engineering Department, U.E.T Taxila, Taxila, Pakistan.

(Received: 26 February 2024, Accepted: 08 March 2024)

(4th International Conference on Innovative Academic Studies ICIAS 2024, March 12-13, 2024)

ATIF/REFERENCE: Ammar, M., Khurshid, M. A. & Mehmood, T. (2024). A T-type LLC Resonant DC-DC-AC Three Port Converter. *International Journal of Advanced Natural Sciences and Engineering Researches*, 8(2), 160-170.

Abstract – Three-port converters (TPC) have become a popular study issue over the past few years due to their potential uses in from renewable sources and battery backup with great power efficiency. This article proposes a bi-directional three-port T-type LLC resonant DC-DC-AC converter to perform soft switching on light loads and in a wide voltage ratio range, to reduce reactive circulating current. This research analyzes the Grid-Connected Photovoltaic (PV) system and battery backup system with the use of a Three-port DC-DC-AC converter (TPC). The purpose of this research is to propose a high-efficiency isolated DC-DC-AC three-port converter (TPC) for home photovoltaic battery systems. The TPC is developed from a DC-AC DAB converter. Its DC-side shares the full-bridge design that offers two bi-directional dc ports, but its AC-side permits direct AC-load connection through a T-type half-bridge arrangement. The suggested TPC enables single-stage power conversion and a significant amount of control degrees of freedom (CDF) while having a smaller number of components due to shared branch design and T-type architecture. The TPC can retain high efficiency. The MATLAB/SIMULINK simulation validates the effectiveness of the proposed topology.

Keywords – Three-port converters (TPC), Photovoltaic (PV), Control degrees of freedom (CDF), Dual active Bridge (DAB), Inductor-inductor-capacitor (LLC)

I. INTRODUCTION

Three-port converters have garnered significant attention now a days due to their versatile use in various energy generation systems. These converters possess three input/output ports, making them suitable for interfacing multiple energy sources or storage elements, such as renewable energy sources, batteries, and the grid. This literature review aims to provide an overview of the key aspects of three-port converters, including topologies, control strategies, applications, challenges, and recent developments.

Three-port converters come in various topologies, each designed to address specific energy system requirements. Among the commonly studied topologies is T-type topology. The T-type topology is renowned for its ability to connect two energy sources and a load simultaneously. It offers the advantage of reduced component count and enhanced efficiency.

Three-port converters find applications in various fields, including: In photovoltaic systems, three-port converters enable the integration of solar panels, batteries, and the grid. They enhance energy harvesting efficiency and grid interaction. In EVs, three-port converters facilitate the connection of the battery, DC link, and motor drives. This enhances the vehicle's powertrain efficiency and regenerative braking capability.

Three-port converters are crucial in hybrid systems that combine multiple energy sources, such as photovoltaic panels, wind turbines, and fuel cells. They enable seamless energy flow management in these complex systems.

To produce a rectified sinusoid voltage, the independent PV system in this study uses a three-port connection. This proposed [1] solar power system has a compact size and only a few conversion steps, making it an excellent choice for PV systems needing a small, affordable power management solution. This method is not suited for high-power applications since the rectified signal demands the interface to handle twice average power at its peak output. Their output signals can be paralleled though to increase power and add redundancy.

Additionally, their inputs can be linked to distributed solar energy sources to maximize the power extracting from each PV panel individually, which would ultimately boost the solar energy extracting for the entire system. The three-port connection is achieved through the modification of the conventional half-bridge DC to DC converters. As a result, it offers a simple power design stage for engineers in practice. Nevertheless, the layout of the control system is highly intricate, as it necessitates a description of the dynamic behavior of the converter and an in-depth study of a multiloop control design.

In this study [2], a soft-switched TPC (three port converter) for solar power and battery is proposed. The proposed TPCs has advantages over the currently available soft-switched TPC in that it uses fewer switches and each of them can be switched on in a zero-voltage switching state. Another study [3] introduces a three-port inverter for PV panels, which links them to a power grid. The output power fluctuates at double line frequency in a grid-connected solar panel whereas its input power remains constant over the line-frequency interval. A traditional flyback inverter is equipped with a series power decoupling circuit that uses thin-film capacitor to manage the difference between its input power and output power. Therefore, compact, long-lasting thin film capacitors are used in place of commonly used, electrolytic capacitors. The suggested inverter can decouple the input as well as output powers and can also extract the greatest amount of power from solar panels and provide low THD (total harmonic distortion) sinusoidal electrical current to the output. The inverter primary switch is shared by the designed power decoupling circuitry.

In this study [4], a three-port, DC/AC converter is presented. This converter intends to connect a set of batteries, a source of clean energy, with a three-phase power utility. A battery and utility interface can transfer electricity between them in both directions. It has triple active bridges, a triple-winding HF AC-link transformers, and an LC circuit. This arrangement is simpler and more dependable than the traditional three-port converter because it only has one LC circuit. Phase shift control(PSC) using a high, constant switching frequency(f_s) is the suggested modulation. On AC-side, duty ratio is now introduced based on

utility phase. To regulate the transfer of reactive and actual power, an additional phase angle is provided. This configuration can be viewed as the combination of both a three-phase converter with a DAB converter. Due to the quasi-sinusoidal as well as trapezoidal waves created by the currents that flow through the windings of a transformer, which allows the low rms as well as maximum current magnitudes. This work proposes a brand-new, three-port three-phase isolated design. Full bridges on DC side, a matrix converter at AC side and a HF transformer is used, and the AC port has a LC circuit.

This proposed structure has fewer components because it only has a single LC tank. Conversion in a single stage, reactive as well as real power control, power flow, greater switching frequency, reduced device stresses, fewer elements, superior efficiency, and reduced rms and maximum currents are all characteristics of proposed converter. The topologies shown in [1],[7],[8] use dual-stage architecture, a straightforward in structure and easy to execute, to carry out this conversion. Multi-stage conversion of power, nevertheless, leads to large component count, increase capacitance of dc-bus, and also lowers the power efficiency.

TPCs in [2], [3] employed a "cyclo-converter-type" construction to directly link the high frequency AC voltage and Line frequency AC voltage in order to perform single-stage conversion. In theory, this type of organization is straightforward and only needs a few active components. But this leakage inductance causes surges in voltage on the switches, makes it more costly and decreasing their effectiveness. Various isolated DAB based converter designs were presented [4]– [6] to address this intrinsic issue.

The AC side of DAB can handle the AC voltage by swapping out each of the switches on each side of converter DAB with switches. This type of TPC works at low switching losses as well as small voltage spikes because of the ZVS operation of the DAB construction and the capacitor which are coupled together with the switches through parallel combination. These TPCs nevertheless needs multi-winding transformer and many switches, which result in substantial loss of power and expensive prices. The TPC suggested in [9] utilized half bridge architecture on the AC-side as a replacement for of full bridge architecture to decrease the total number of switches and thus increasing the efficiency. On the DC side, another DC port was built using the branch sharing technique without the use of additional switches.

The TPC in [10] similarly utilized a branch sharing technique to lower the switches. DAB based full-bridge converter, this TPC shares its switches on DC side with a boost converter and full bridge with a converter on AC side, enabling direct connection of AC load. As described above, it can be inferred that TPC converter with shared branch is more advantageous in terms of efficiency, price, and power density for applications in homes.

These cutting-edge technologies still have several problems, though, which lower their efficiency. Their AC-side structures have a few flaws built right in, to start. If an anti-series switches full-bridge circuit is used (see the TPCs in [4]–[6], [9]), a large switch count will lead to significant losses. On the opposite side it can produce two level High frequency AC voltage only if a half bridge design is used on AC side of the converter (see the TPCs in [7], [10]).

For the half bridge structure, the Control of degree of freedom (CDF) of the phase shift ratio is compromised. Furthermore, it is acknowledged that the phase-shift ratio is crucial in enhancing the effectiveness of DAB converters [11]. Therefore, the efficiency is limited by insufficient Control of degree of freedom (CDF) of the half bridge. The branch sharing strategy will lead to modulation coupling problems, wasting Control of Degree of Freedoms, and decreasing efficiency, which is another problem. A duty cycle of the shared branch is typically used to control flow of power between DC-DC side of converter, whereas phase-shift ratio among them is typically used to regulate the power flow between dc-ac side of the converter. Though, there will be interference between the phase shift ratio and duty cycle, leading to a problem of modulation coupling.

According to [1], [2], [3], and [15], the modulation techniques for branch shared TPC typically manage to fix their dc side phase shift ratio at 50 %. Less Control of degree of Freedom (CDF) as a result of a constant phase shift ratio lower the TPC effectiveness. The TPC in [7] controls the dc/dc stage using the switching frequency(f_s) rather than the pulse width (PWM) to prevent the waste of CDF. However, leakage inductance meeting the transmission of power can only partially ensure efficiency due to the significantly fluctuating frequency. This proposed scheme seeks to propose a constant frequency modulation technique without Control of degree of Freedom (CDF) waste to increase efficiency.

Another problem is that dc-dc stage inductor current may impair the DC-side Zero Voltage switch (ZVS) performance, lowering efficiency. The DC/DC stage of a branch shared TPC is often comparable as two parallel buck-boost converters. The one directional current on the dc/dc inductor will cause ZVS losses if converter runs in (CCM)continuous conduction mode, as detailed in [12], [13], and [14].

II. MATERIAL AND METHOD

Due to the potential applications of TPC (three-port converters) in energy storage system like batteries and in renewable and alternate energy systems, they have grown in popularity as a study area recently. In addition to the availability of an AC port, dc-dc-ac TPC [1]–[6] are more desirable than dc-dc-dc TPCs for the production of domestic power. Depending on whether a transformer is present, the dc-dc-ac TPC can be divided into two categories such as non isolated and isolated variants. The lack of transformer usually results in step up ratio limitations for non-isolated TPC [7]– [9]. Galvanic isolation is furthermore frequently required for domestic applications for safety concerns, making isolated TPC more appropriate.

DAB based TPCs suffer from some issues which are mentioned as:

- 1) first, their ac-side topologies have few inherent defects regarding the switches of DC as well as of AC side switches.
- 2) The branch sharing strategy will lead to modulation coupling problems, which decreases its efficiency.
- 3) The DC side ZVS (Zero voltage switching) performance may suffer from the dc-dc inductor currents, which would lower efficiency.

An isolated TPC with an appropriate modulation technique is developed in order to accomplish the three goals described above and finally realize high efficiency. These three areas represent the study's primary contributions:

- 1) By including a pair of switches on the AC-side of a half bridge DAB based converters, a T-type topology is created. Both switches just have to endure 50% of the AC voltage in order to prolong one CDF. As a result, higher efficiency may be attained without the need of bulky switches capable of handling the entire AC voltage by using a greater number of variables.
- 2) Both type of conversions is suggested using a PWM with TPS modulation technique. A cycle substitution method that preserves the total number of CDFs is used to address modulation coupling problem. According to these adequate CDFs, TPS modulation may be used to enhance the dc-ac rms.
- 3) On the DC-DC conversion, a connected inductor is used in place of two separate dc-dc inductors. A coupled inductor produces a high level of magnetic integration. Additionally, magnetic inductance may be utilized to reduce the current ripple on battery port, whereas its leaking inductance may be employed to assist the ZVS performance.
- 4) At lower voltage conversion ratio M (M less than 1), LLC resonant architecture is employed to boost efficiency and attain ZVS condition. Based on voltage conversion ratio as well as the load circumstances, three controlling parameters—switching frequency (f_s), duty cycle (D), as well as phase shift—have been modified

III. MATHEMATICAL MODELING OF T-TYPE LLC RESONANT THREE-PORT CONVERTER

The proposed schematic converter is a modified DAB converter. DAB converter is modified, first to create an additional port on DC-side. Secondly, LLC circuit is introduced on primary side of the transformer. A combination of coupled inductor and full bridge circuitry make up dc side of the converter. The full bridge is made up of two half bridge circuits named as, HB1 and HB2, that are paralleled with a DC power source (such as a solar panel on Port 1. The linked inductors attach to the halfway points of HB1 and HB2. Regarding the AC side topology, to adjust the line voltage (V_{ac}) on Port C, the active switches Q_1 – Q_4 along with two High Frequency capacitors C_2 and C_3 form a bi-polar half bridge architecture. The center points of each switch branch and the corresponding capacitor branch are linked by a set of anti-series switches Q_5 and Q_6 . Switches Q_5 and Q_6 can only endure 50% of the AC voltage since C_2 and C_3 divide the V_{ac} to two equal portions. A High-Frequency transformer of 1:n turn ratio and an inductor represented are used to serve as a power flow channel that connects the DC-side and the AC-side while establishing isolation.

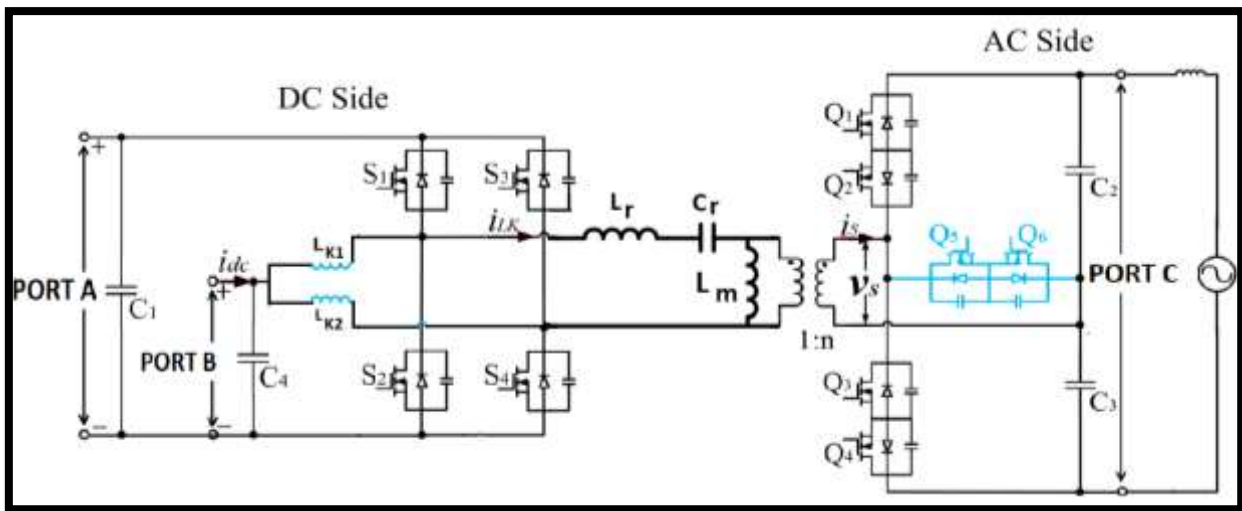


Figure 1. Proposed three-port (TPC) LLC resonant isolated bidirectional.

Typically, control of power flow is used to analyze the multi-port converter's operating principles [3]. Two flows of power, between DC-DC and between DC_AC port, both need to be controlled for the suggested TPC.

1) Control of DC-to-DC port power flow: To make the analysis simpler, the linked inductors L_1 and L_2 are identical to the Y-connected inductors. Following is how they are connected:

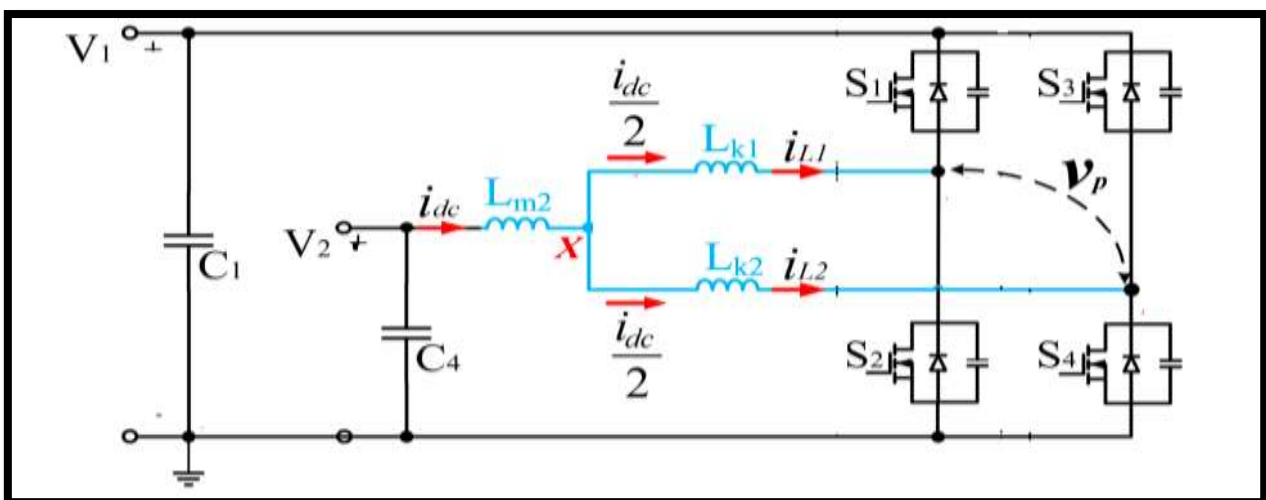


Figure 2. Primary side of proposed converter

$$\begin{cases} L_{k1} = L_1 - L_{m2} \\ L_{k2} = L_2 - L_{m2} \\ L_{m2} = k\sqrt{L_1L_2} \end{cases} \quad (1)$$

where k is the strength of the connection between and. The comparable circuit for a dc-dc circuit is then created (see Fig. 2). The voltage fluctuations on Ports A and B are disregarded in the description that follows because it is based on this analogous circuit.

It is necessary to describe the relationship between voltage and current of the DC-DC stage before illustrating the DC-DC power control flow theory. The dc-dc power flow is controlled by an inductor current, which is made up of i_{l1} and i_{l2} . Computation of inductor currents is as follows:

$$L_{k1} \frac{di_{L1}(t)}{dt} = v_{XN} - v_{AN} \quad (1)$$

$$L_{k2} \frac{di_{L2}(t)}{dt} = v_{XN} - v_{BN} \quad (2)$$

$$L_{m2} \frac{di_{dc}(t)}{dt} = V_2 - v_{XN} \quad (3)$$

It may be shown in Fig. 2 that $i_{dc}(t) = i_{L2}(t) + i_{L1}(t)$. Consequently, if we suppose $L_{k1} = L_{k2}$ and after adding (2) and (3), we get:

$$L_{k1} \frac{di_{dc}(t)}{dt} = 2v_{XN} - (v_{AN} + v_{BN}) \quad (5)$$

By changing from (4) into (5), we get at

$$\left(L_{m2} + \frac{L_{k1}}{2} \right) \frac{di_{dc}(t)}{dt} = V_2 - \frac{v_{AN} + v_{BN}}{2} \quad (6)$$

The voltages are determined by the switching states of $S_1 - S_4$ -. If the switching signals and voltages can be expressed as:

$$\begin{cases} v_{AN} = V_1 \times s_1(t) \\ v_{BN} = V_1 \times s_3(t) \end{cases} \quad (7)$$

$$\left(L_{m2} + \frac{L_{k1}}{2} \right) \frac{di_{dc}(t)}{dt} = V_2 - V_1 \cdot \frac{s_1(t)+s_3(t)}{2} \quad (8)$$

The VI relationship of the dc-dc stage is described by equation (8). When applied to equation 8 at steady state, the volt second balance reveals further details about the dc-dc stage's workings as follows:

$$0 = V_2 - V_1 \cdot \frac{\bar{s}_1(t)+\bar{s}_3(t)}{2} \quad (9)$$

$\bar{s}_1(t)$ and $\bar{s}_3(t)$ are the average of period of $s_1(t)$ and $s_3(t)$.

$$V_2 = D_s V_1 \quad (10)$$

Eq. 10 shows that the DC-DC stage's steady state voltage relationship is identical as a typical buck-boost converters. As a result, the pulse width of $s_1(t)$ and $s_3(t)$ controls the supply of dc-dc power.

The ZVS (zero voltage switching) of the dcdc stage thus relies on the changes of I_{l1} and I_{l2} across a switching cycle, which requires more analysis. If we use the following definitions for $I_{l1}(t)$ and $I_{l2}(t)$ circulation current I_{cir} :

$$i_{cir}(t) = i_{L2}(t) - i_{L1}(t) \quad (11)$$

$$\begin{aligned} i_{L1}(t) &= \frac{i_{dc}(t) - i_{cir}(t)}{2} \\ i_{L2}(t) &= \frac{i_{dc}(t) + i_{cir}(t)}{2}. \end{aligned} \quad (12 \& 13)$$

The analysis may be made simpler by leaving out the electrical current ripple because the magnetic inductor is so huge. Consequently, may be roughly described as a dc flow whose amplitude varies exclusively on the mean dc-dc power flow.

$$L_{k1} \frac{d(i_{L2}(t) - i_{L1}(t))}{dt} = L_{k1} \frac{di_{cir}(t)}{dt} = v_{AN} - v_{BN} \quad (14)$$

Integrating both sides of equation 14, we get

$$i_{cir}(t) = \frac{1}{L_{k1}} \times \int (v_{AN} - v_{BN}) dt = \frac{1}{L_{k1}} \times \int v_p dt \quad (15)$$

where is the primary voltage on the high frequency transformer, which is the voltage difference among nodes A and B. Since the integral is 0, equation (15) states that the mean value of $i_{cir}(t)$ is zero. On the other hand, as seen in Fig. 3, the instantaneous amount varies with.

$i_{L2}(t)$ and $i_{L1}(t)$ can be inverted at the switching time by constructing suitable L_{k1} and L_{k2} , which facilitates ZVS. Though a lower value leads to greater ZVS condition, it also produces larger rms values on $i_{L2}(t)$ and $i_{L1}(t)$, which raises conduction losses. The linked inductor can help regulate the dc-side ZVS while reducing the battery port current ripple, as was determined from the article above.

IV. LLC RESONANT TOPOLOGY

On the primary side of the transformer, the input capacitor C1 stabilizes half of the input voltage, which is depicted in Fig. 1 of the proposed topology. Half of the output voltage ($V_o/2$) is stabilized on the other side of the transformer by output capacitors C2 and C3, both are of same capacitance value. Lr (Resonant inductance), Cr (resonant capacitor), and Lm (magnetising inductance) combine to create an LLC resonant circuit. Vab voltage that exists between terminal a and b serves as the resonant tank's input.

V. THEORETICAL STUDY

There are forward and backward operations included in this theoretical analysis. Also included is the ZVS (zero voltage switching) analysis of both procedures. Fig. provides the formulas for the equations used in simpler circuits.

Here,

Z_o is the characteristic impedance,

F is the normalized frequency,

f_o is the resonant frequency,

λ is the inductance ratio,

R_{ac} is the AC equivalent reflected load resistance, and

Q is the quality factor.

$$Z_o = \sqrt{\frac{L_r}{C_r}}$$

$$F = \frac{f_s}{f_o}$$

$$f_o = \frac{1}{2\pi\sqrt{L_r C_r}}$$

$$\lambda = \frac{L_m}{L_r}$$

$$R_{ac} = \frac{2n^2}{\pi^2}$$

$$R_o = \frac{Z_o}{Q},$$

$$Q = \frac{Z_o}{R_{ac}}$$

The calculations employed f indices for the forward and r indices for the reverse power flow analysis.

VI. RESULTS

In this section, we present the results of the simulation conducted in MATLAB/Simulink for the proposed T-type LLC resonant DC-DC-AC three-port converter. The simulation aimed to evaluate the performance of the converter under various operating conditions, including three-phase input to the rectifier, output of the AC side, and the bidirectional flow of power from AC to DC port (rectifier).

The simulation results demonstrate the effective rectification of the three-phase input voltage by the rectifier module of the converter. The rectifier converts the AC input voltage into a pulsating DC waveform, which serves as the input to the subsequent DC-DC conversion stage. The rectified output voltage exhibits low ripple and distortion, indicating smooth rectification and efficient power transfer from the AC source to the converter.

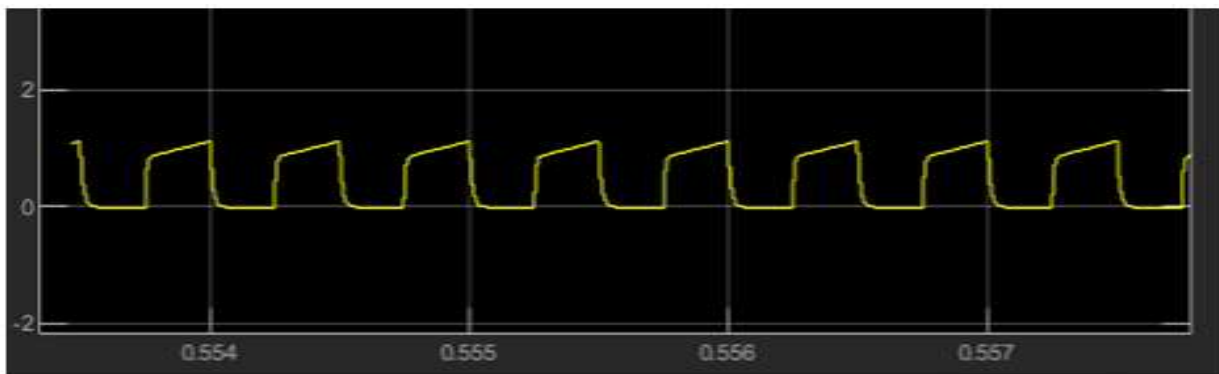


Figure 3. Inductor current waveform i_{LK}

The AC side output of the converter exhibits a sinusoidal waveform with controlled amplitude and frequency, reflecting the successful conversion of the rectified DC input to AC output. The output voltage is regulated within predefined limits, ensuring compatibility with the grid or AC load. The simulation demonstrates the ability of the converter to maintain stable AC output voltage despite variations in the input DC voltage and load conditions.

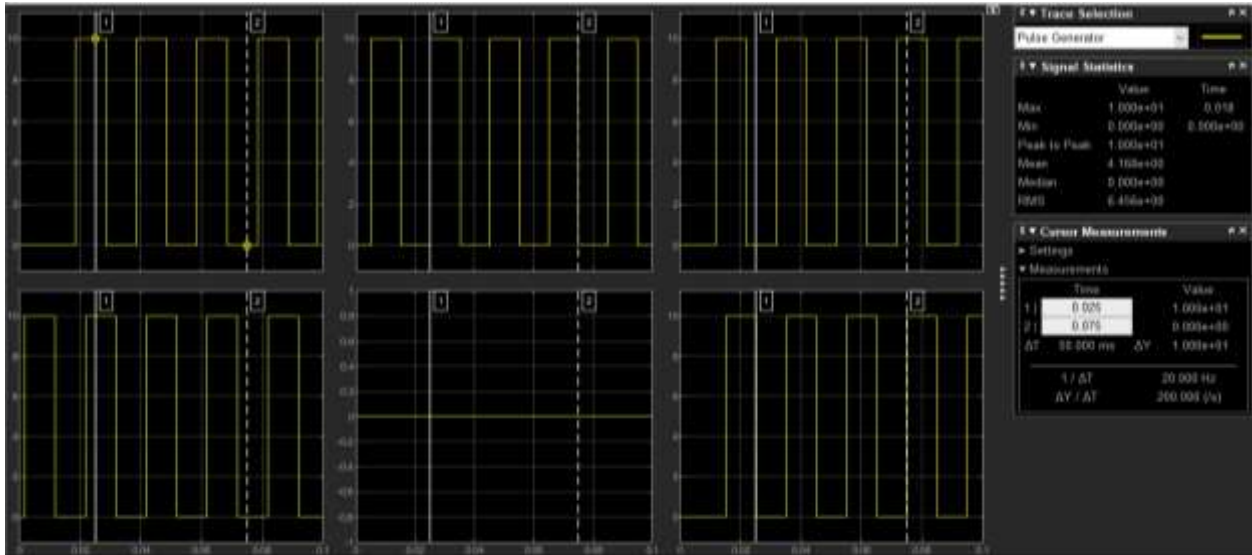


Figure 4. Switching Pulses

The bidirectional flow of power from the AC to DC port of the converter is achieved through the rectifier module. During this process, the converter operates in the buck mode, stepping down the AC input voltage to match the desired DC output voltage. The simulation results indicate efficient power transfer from the AC side to the DC port, with minimal losses and high conversion efficiency. Additionally, the converter allows for seamless bidirectional power flow, enabling energy transfer between the AC and DC ports as required by the system.

Table 1. Comparisons of Different Converters

Parameters	The Converter in [6]	The Converter in [7]	The Converter in [8]	Proposed Converter
Topology (PB+SB)	FB+LC+FB	FB+LC+FB	TL+LC+LC+TL	2HB+LLC+T-type
Control Method	FDM	PSM+PWM	PSM+PWM	PWM+PI
Number of Control Variables	4	3	3	4
No. of Primary Switches	4	4	8	4
No. of secondary switches	4	4	8	6
Number of Resonant inductors	1	1	2	1
Number of Resonant Capacitor	1	1	2	1
Cost	Medium	Medium	High	Medium
Switching Frequency	80-117	100	31-70	45.45
Types of switches	SiC+ MOSFETs	MOSFETs	16 MOSFETs	10 MOSFETs
Voltage stress of switches	Vin & Vo	Vin & Vo	0.5Vin & 0.5Vo	0.5Vin & 0.5Vo

Overall, the simulation results validate the effectiveness of the proposed T-type LLC resonant DC-DC-AC three-port converter in facilitating efficient power conversion and bidirectional energy transfer between multiple energy sources. The converter demonstrates stable operation, high efficiency, and robust performance under varying operating conditions, highlighting its potential for real-world applications in grid-connected PV systems with battery backup.

VII. DISCUSSION

The simulation results confirm the feasibility and effectiveness of the proposed converter topology in meeting the objectives of the research. By integrating LLC resonant topology with the T-type architecture, the converter achieves efficient power conversion, reduced switching losses, and improved control over power flow. The bidirectional power flow capability of the converter enables seamless integration of renewable energy sources, such as PV arrays and batteries, with the grid, thereby enhancing the reliability and resilience of the overall energy system. Furthermore, the simulation results provide valuable insights into the performance characteristics of the converter under different operating conditions. The controlled output voltage and low distortion of the AC side output demonstrate the converter's ability to maintain stable grid synchronization and provide high-quality AC power to the load. Similarly, the bidirectional power flow capability of the converter enables effective energy management and optimization of power flow between the AC and DC ports, ensuring efficient utilization of available energy resources.

VIII. CONCLUSION

Overall, the simulation results support the conclusion that the proposed T-type LLC resonant DC-DC-AC three-port converter offers significant advantages in terms of efficiency, flexibility, and reliability compared to conventional converter topologies. The converter shows promise for a wide range of applications, including grid-connected PV systems, microgrids, and electric vehicle charging stations, contributing to the advancement of sustainable energy technologies and the transition towards a more resilient and environmentally friendly energy infrastructure.

REFERENCES

1. Z. Qian, O. Abdel-Rahman, H. Hu and I. Batarseh, "An integrated threeport inverter for stand-alone PV applications," in Proc. IEEE Energy Convers. Congr. Expo., Atlanta, GA, USA, 2010, pp. 1471-1478.
2. J. Zeng, W. Qiao, C. Wei and L. Qu, "A soft-switched three-port singlestage inverter for photovoltaic-battery systems," in Proc. IEEE Energy Convers. Congr. Expo., Montreal, QC, Canada, 2015, pp. 4568-4573.
3. M. Hadi Zare, M. Mohamadian and R. Beiranvand, "A single-phase gridconnected photovoltaic inverter based on a three-switch three-port flyback with series power decoupling circuit," IEEE Trans. Ind. Electron., vol. 64, no. 3, pp. 2062-2071, March 2017.
4. J. Andrade, D. S. y Rosas, D. Frey and J. -P. Ferrieux, "Modified triple active bridge DC/AC three-phase converter with a series-resonant LC circuit on the AC-side," in Proc. IEEE South. Power Electron. Conf., Puerto Varas, Chile, 2017, pp. 1-6.
5. J. U. Ugwuanyi, Y. P. Chan, K. H. Loo and Y. M. Lai, "Three-port ac-dc bidirectional converter with V2G reactive power support," in Proc. IEEE Power Energy Conf. Illinois, Champaign, IL, USA, 2017, pp. 1-7.
6. A. K. Bhattacharjee and I. Batarseh, "Sinusoidally modulated ac-link microinverter based on dual-active-bridge topology," IEEE Trans. Ind. Appl., vol. 56, no. 1, pp. 422-435, Jan.-Feb. 2020.
7. Y. Shi, R. Li, Y. Xue and H. Li, "Optimized operation of current-fed dual active bridge dc-dc converter for PV applications," IEEE Trans. Ind. Electron., vol. 62, no. 11, pp. 6986-6995, Nov. 2015.
8. G. -R. Chen, H. -L. Jou, Kuen-Der Wu and J. -C. Wu, "Single-phase threewire fuel-cell generation system for micro-grid," in Proc. IEEE Conf. Ind. Electron. Appl., Hangzhou, China, 2014, pp. 610-615.
9. A. K. Bhattacharjee and I. Batarseh, "An interleaved boost and dual active bridge-based single-stage three-port dc-dc-ac converter with sine PWM modulation," IEEE Trans. Ind. Electron., vol. 68, no. 6, pp. 4790-4800, June 2021.
10. S. Kurm and V. Agarwal, "Dual active bridge based reduced stage multiport dc/ac converter for PV-battery systems," IEEE Trans. Ind. Appl., vol. 58, no. 2, pp. 2341-2351, March-April 2022.
11. B. Zhao, Q. Song, W. Liu and Y. Sun, "Overview of dual-active-bridge isolated bidirectional dc-dc converter for high-frequency-link powerconversion system," IEEE Trans. Power Electron., vol. 29, no. 8, pp. 4091-4106, Aug. 2014.
12. X. Sun, Y. Shen, Y. Zhu and X. Guo, "Interleaved boost-integrated LLC resonant converter with fixed-frequency PWM control for renewable energy generation applications," IEEE Trans. Power Electron., vol. 30, no. 8, pp. 4312-4326, Aug. 2015.

13. H. Wu, J. Zhang, X. Qin, T. Mu and Y. Xing, "Secondary-side-regulated soft-switching full-bridge three-port converter based on bridgeless boost rectifier and bidirectional converter for multiple energy interface," *IEEE Trans. Power Electron.*, vol. 30, no. 7, pp. 4847-4860, July 2016.
14. Y. Shi, R. Li, Y. Xue and H. Li, "Optimized operation of current-fed dual active bridge dc-dc converter for PV applications," *IEEE Trans. Ind. Electron.*, vol. 62, no. 11, pp. 6986-6995, Nov. 2015.